

MODELING OF CAVITATION FLOW ON NACA 0015 HYDROFOIL

Jaroslav Štigler*, Jan Svozil*

This paper is concerning with simulations of cavitation flow around the NACA 0015 hydrofoil. The problem is solved as the multi-phase and single-phase model of flow, for two different impact angles and for two different densities of computational net. The attention is focused on the comparison of single-phase and multi-phase results.

Keywords: cavitating flow, multiphase flow, NACA 0015

1. Introduction

Modeling of cavitation flow as a multi-phase flow is a complex problem which does not lead to satisfying results especially when the cavitation is modeled as 3D. Therefore in the engineering practice cavitation flow is often modeled as a single-phase flow, where the cavitation area is handled as an area with the pressure lower then the vapor pressure. This approach always leads to the result, and the requirement of computer time is many times lower in comparison with multi-phase flow models. Moreover the steady solution of multi-phase flow model may not be found at all due to the unsteady nature of cavitation flow.

The object of this paper is a comparison of single-phase and multi-phase models of cavitating flow with different densities of computational nets and different versions of a solver. This comparison is made by means of 2D flow round the NACA 0015 hydrofoil for two different impact angles. The solution will be done for two different versions of Fluent software 6.3.28 and 6.4.

2. Nomenclature

Mark	Title	Unit
c_∞	Freestream velocity	[m/s]
F_z	Uplift force on the hydrofoil	[N]
C_z	Uplift coefficient	[-]
C_p	Pressure coefficient	[-]
L	Chord lengh	[m]
p_∞	Freestream pressure	[Pa]
p_{vap}	Vapor pressure	[Pa]
p_x	Pressure in the certain location on the hydrofoil	[Pa]
L_c	Cavity lengh	[-]
ϱ	Density of fluid	[kg/m ³]
σ	Cavitation number	[-]

* doc. Ing. J. Štigler, Ph.D., Ing. J. Svozil, Technical University of Brno, Faculty of Mechanical Engineering, V. Kaplan's Department of Fluid Engineering, Technická 2, Brno

3. Boundary and initial conditions

The calculation has been made for the NACA 0015 hydrofoil with 0.115m the length of chord. Further parameters of solution are listed below.

Title	Mark	Value	Unit
Reynolds Number	Re	577 000	$[-]$
Temperature	t	25	$[^{\circ}\text{C}]$
Velocity inlet	c_{∞}	4.5	$[\text{m s}^{-1}]$
Length of chord	L	0.115	$[\text{m}]$
Turbulence intensity		10	$[\%]$
Vapor pressure	p_{vap}	3 133	$[\text{Pa}]$
Density of water	ϱ	997	$[\text{kg m}^{-3}]$

4. Computational net

The Fig.1 and the Fig.2 shows the fine and the raw computational net used in the simulations. Grids in both cases are mapped.

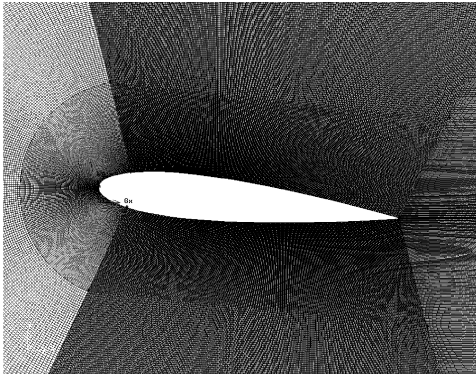


Fig.1: The fine computational net (538 764 cells)

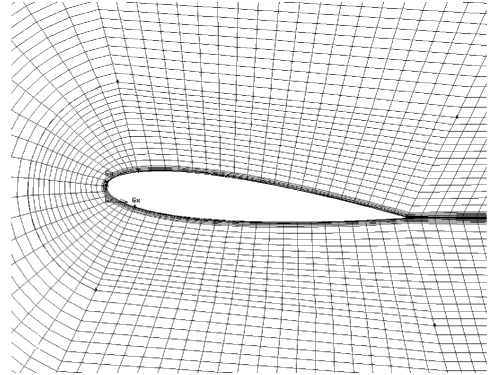


Fig.2: The raw computational net (16 087 cells)

5. Results And the Discussion

Most of characteristics are drawn as a function of cavitation number. This number expresses how much the free stream pressure energy exceeds the vapor pressure energy. Difference of these pressure energies is related to the free stream kinetic energy. Cavitation number is expressed as

$$\sigma = \frac{p_{\infty} - p_{\text{vap}}}{\frac{1}{2} \varrho c_{\infty}^2} . \quad (1)$$

The free stream pressure p_{∞} is taken as an average value from three points. Their positions are outlined in the Fig. 3.

The uplift coefficient is defined in this way

$$C_z = \frac{2 F_z}{c_{\infty}^2 \varrho L} . \quad (2)$$

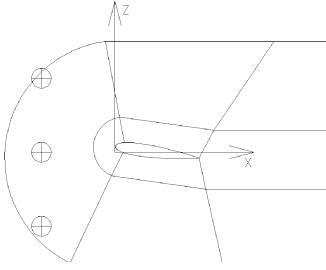


Fig.3: Layout of the points for the free stream pressure calculation

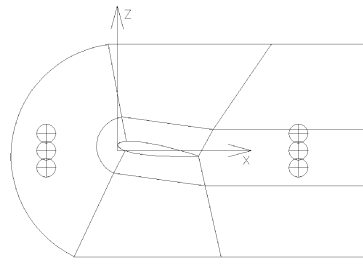


Fig.4: Layout of points for pressure difference calculation

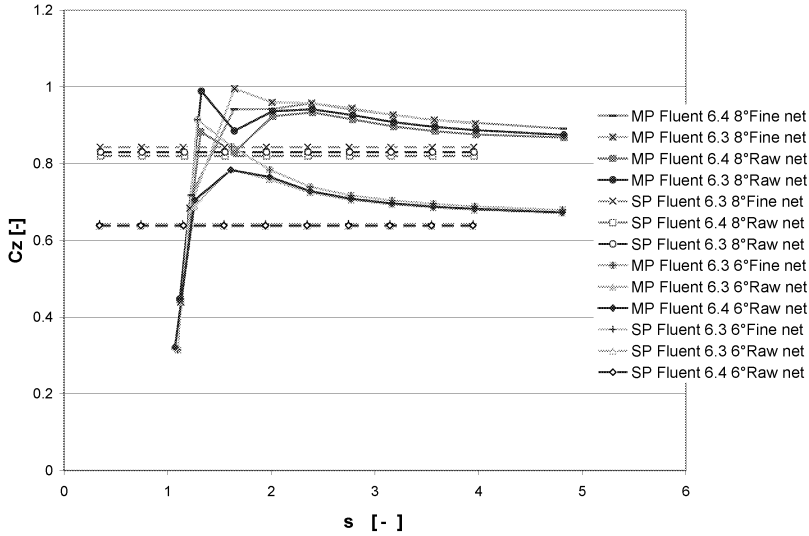


Fig.5: Uplift coefficient for both angles of attack, 6° and 8°, and for single-phase (SP) and multi-phase (MP) model of solution

The comparison of uplift coefficient for the single-phase and the multi-phase solution is shown in Fig. 5. Each shade of gray is used for one combination of angle of attack and the version of solver.

Multi-phase models are signed by full lines and single-phase models by dashed lines. The difference between these two models is increasing with the cavitation number decreasing. The multi-phase model solution is converging to the single-phase model solution in the area of non-cavitating flow ($\sigma > 4$).

The single-phase model solution is not sensitive to the cavitation number and the value of uplift coefficient remains constant.

Differences between different densities of computational net are negligible.

6. The dimensionless pressure difference

The dimensionless pressure difference is calculated as

$$\Delta p = \frac{p_1 - p_2}{\frac{1}{2} \rho c_\infty^2} . \quad (3)$$

The previous expression in fact is a definition of loss coefficient for the flow singularity with the assumption of constant velocity and as such it can be derived from the Bernoulli equation.

Pressures p_1 and p_2 are taken as an average values of 3 points. Their location at the inflow and outflow area is shown on next Fig. 4.

Differences between both versions of solver and different attack angles are negligible. But better agreement with experimental data could be seen for the fine computational net, multiphase model and angle of 8° of attack than for the other solutions. It is apparent

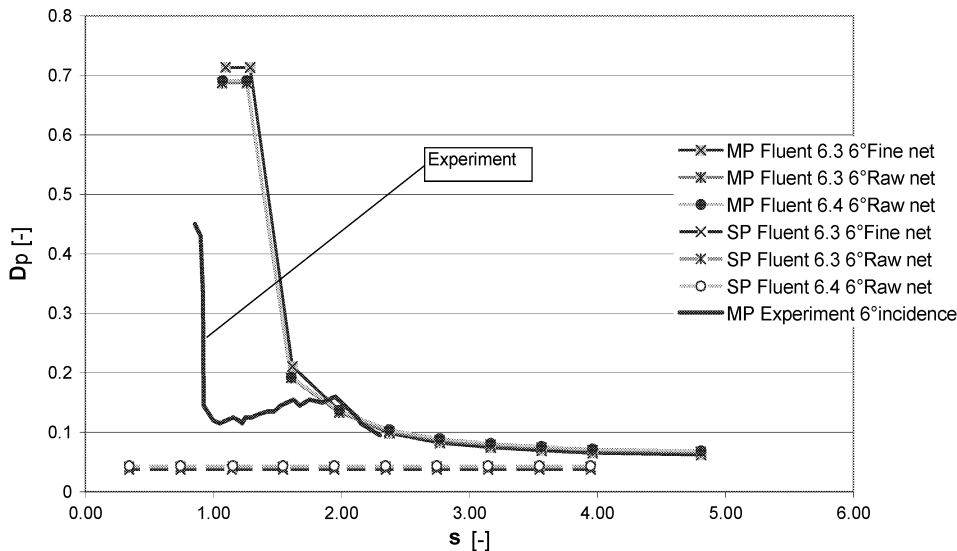


Fig.6: The comparison of pressure difference for 6° attack angle, various densities of computational net, solvers and experiment

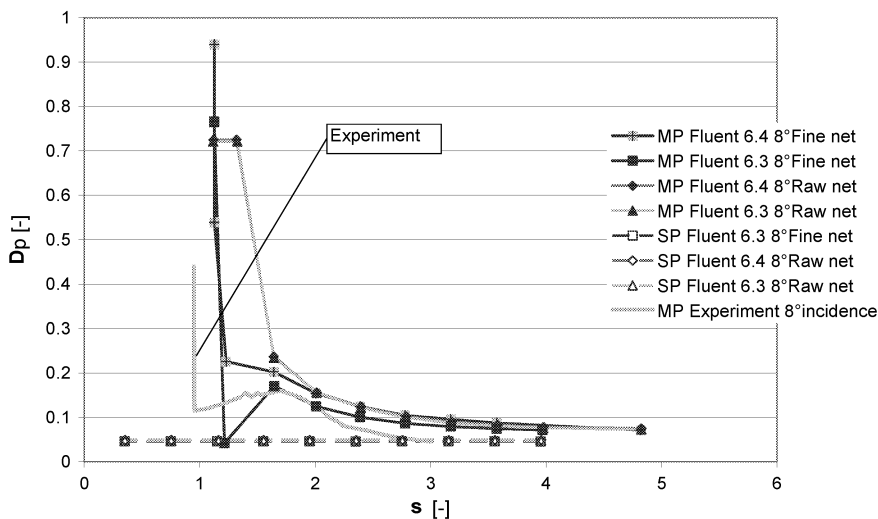


Fig.7: The comparison of pressure difference for 8° attack angle, various densities of computational net, solvers and experiment

that the pressure difference is independent of cavitation number. This is the same result as for the uplift coefficient. Some differences between the single-phase and the multi-phase solution occur in the regime of non-cavitation flow ($\sigma > 4$). But it seems that the multiphase solution is converging to the single-phase solution with σ increasing.

7. The cavity length

Different definitions of cavity area have to be used for the single-phase and the multi-phase model of solution because of different nature both types of flows.

The cavity area for the case of single-phase model is defined as an area of pressure lower than the vapor pressure.

The cavity area for the case of multi-phase-model is defined as an area where the vapor appears. The border of this area is given by the equilibrium of both phases. It means that the volumetric part of liquid phase and vapor phase are equal in the net cell.

The cavity area at the single-phase model is defined in unambiguous way. Meanwhile the cavity area in case of multi-phase model depends on proportion of both phases.

The comparison of CFD results and experiment is shown in the Fig. 8 and the Fig. 9.

Experimental data were gained from [1] Rapposelli (2003). The cavity length is not given as a single line in dependence on the cavitation number. It is given as a range between minimal and maximal cavity length value.

The cavity area, in the case of single-phase flow model, is strongly underestimated in comparison with experimental data. In the case of multi-phase flow model the cavity area corresponds rather well with experimental data. It is closer to the maximal cavity length in the area of low cavity numbers. For higher cavity numbers it is below the minimal cavity length. It is possible to say that the solution with the multiphase model is in the good agreement with measurements.

The comparison of the cavity size and it's shape for the multi-phase and the single-phase models is outlined in the Fig. 10. Both cases are solved with corresponding boundary

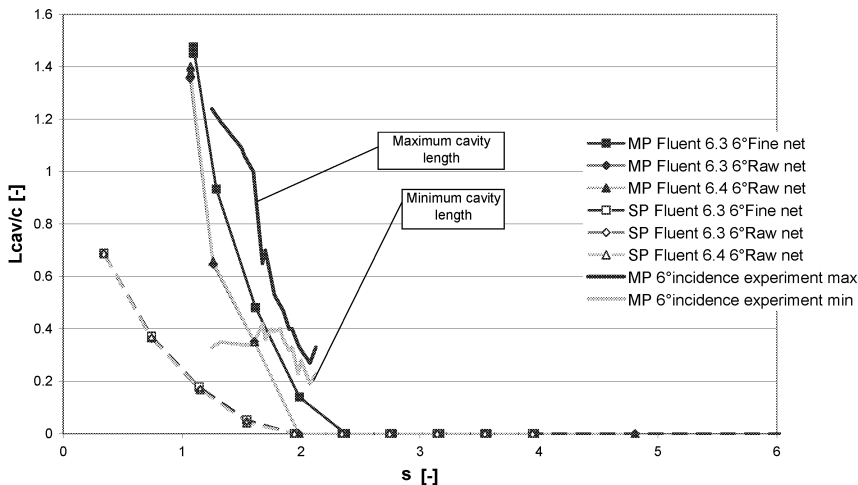


Fig.8: The cavity length for the angle of attack 6° , both version of solver and both densities of computation net

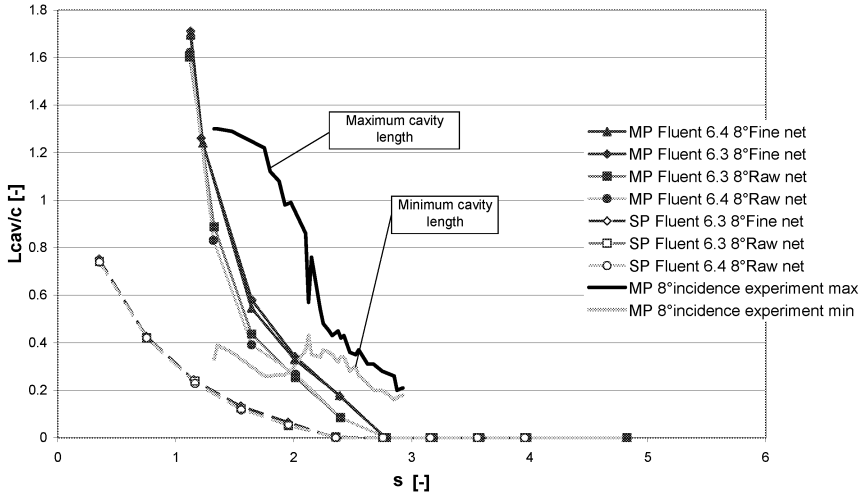


Fig.9: The cavity length for the angle of attack 8° , both versions of solver and both densities of computation net

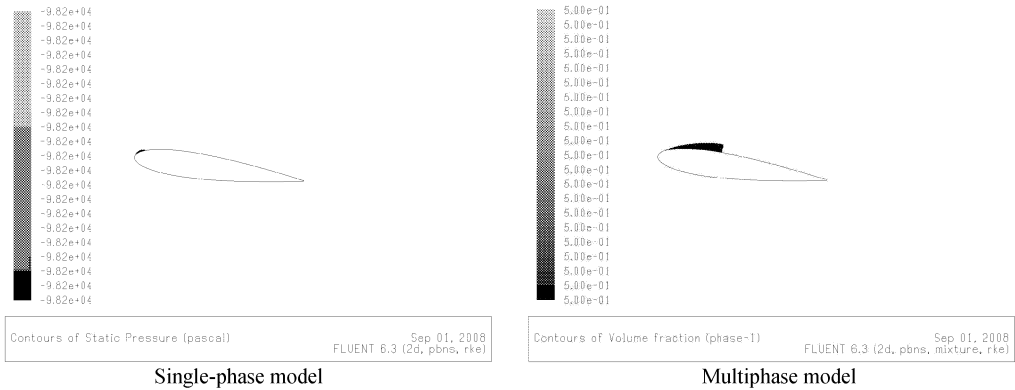


Fig.10: Cavity area for Fluent 6.3, angle of attack 8° and $p = -78 \text{ kPa}$

conditions and the solver version. Despite this the shape and the size of cavity area are dramatically different.

8. The pressure coefficient

The pressure coefficient is defined as

$$C_p = \frac{p_x - p_\infty}{\frac{1}{2} \rho c_\infty^2}.$$

It expresses the pressure distribution on the hydrofoil. This quantity is more sensitive to the cavitation occurrence than the above mentioned definition of cavity area. The distribution of C_p on the hydrofoil for the single-phase and the multi-phase model is very similar for non-cavitating flow. The characteristic shape of this curve is shown in the Fig. 11.

The beginning of cavitation is apparent in Fig. 12. The influence of cavitation on the distribution of C_p is apparent from the Fig. 13. This characteristic deformation of C_p behavior

can be observed only in case of multi-phase model, meanwhile the C_p distribution in case of single-phase model remains indifferent to any cavitation occurrence.

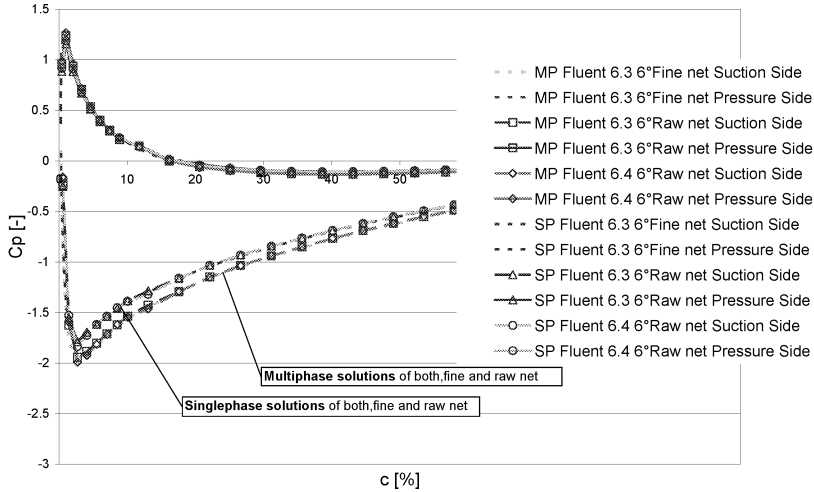


Fig.11: The pressure coefficient for the output pressure -66 kPa and the angle of attack 6°

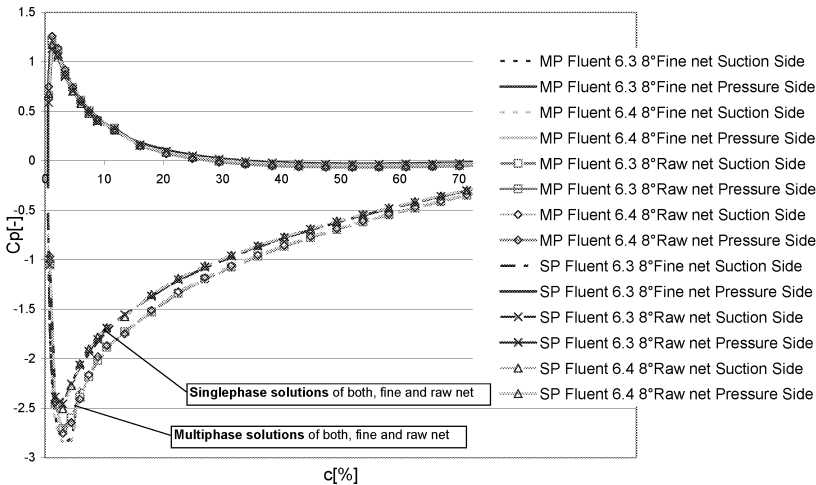


Fig.12: The pressure coefficient for the output pressure -66 kPa and the angle of attack 8°

The characteristic deformation of C_p distribution is given by fact, that the pressure in cavity remains constant. The comparison of solution with the fine and raw computational net shows the another phenomenon which appears at the end of cavity. The pressure increasing at the cavity end in case of fine computational net is higher than in case of raw computational net. It seems that there is the flow separation at the end of cavity in case of solution with the fine computational net. This situation is shown in the Fig. 14. The problem is that this phenomenon appears only for the solution with some cavity number. It needs more detailed investigation for the cavitation numbers between the first occurrence of cavitation and the case when the cavity area is bigger than the length of profile chord.

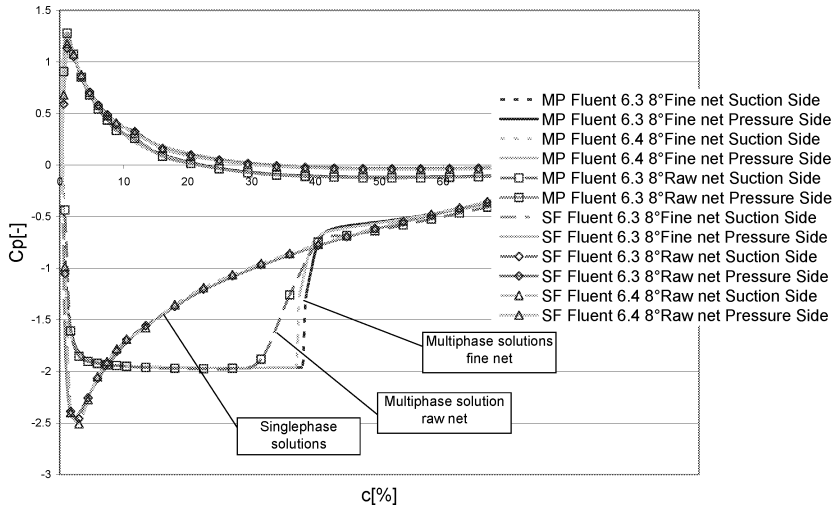


Fig.13: The pressure coefficient for the output pressure -78 kPa and the angle of attack 8°

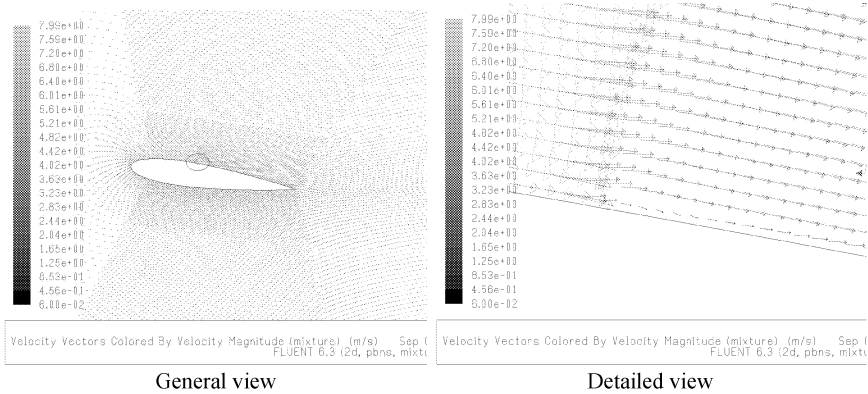


Fig.14: Velocity field for the output pressure -78 kPa and the angle of attack 8°

Also the difference between the fine and raw computational net and the slight difference in the solution between different versions of solver can be found in the Fig. 12 and the Fig. 13.

9. Conclusion

Using the single-phase model for the modeling of cavitating flow leads to errors which are increasing with the cavity number decreasing. The size and the shape of single-phase cavity area is significantly different from those we obtain from the multi-phase model and also the cavity length varies due to these differences.

Differences between different versions of solver are not significant.

Differences in solution between fine and raw computational net are negligible. Difference appears only at the end of cavity for multiphase solution. The need of computer time for the fine net was many-times higher, and moreover for low cavity numbers ($\sigma < 1.5$) the stationary solution was not found at all.

Acknowledgement

Authors are grateful to the Ministry of Industry and Trade of the Czech Republic for funding this research under project with registration number 2A-1TP1/108 and Ministry of Education, Youth and Sports for founding this research under project with registration number MSM0021630518.

References

- [1] Rapposelli E., Cervone A., Barmanti C., Agnostine L.: Thermal Cavitation Experiments on a NACA 0015 hydrofoil, In Proceedings of FEDSM'03, 4TH ASME_JSME Joint Fluids Engineering, Conference July 6–11, ASME, Honolulu Hawaii, USA, 2003

Received in editor's office: September 23, 2008

Approved for publishing: November 6, 2008

Note: This paper is an extended version of the contribution presented at the conference *Hydroturbo 2008* in Hrotovice.